Simulation of Foot-Mounted IMU Signals for the Evaluation of PDR Algorithms

Francisco J. Zampella, Antonio R. Jiménez, Fernando Seco, J. Carlos Prieto, Jorge I. Guevara
Centre for Automation and Robotics (CAR). Consejo Superior de Investigaciones Científicas (CSIC)-UPM.
Ctra. Campo Real km 0.2, 28500 La Poveda, Arganda del Rey, Madrid, Spain.
Email: francisco.zampella@csic.es
Web: http://www.car.upm-csic.es/lopsi/

***Abstract*—A common problem in the evaluation of *Pedestrian Dead Reckoning* (PDR) algorithms is the determination of a good ground truth . Some authors propose the use of external motion capture systems, however, their setup, complexity, synchronization and limited coverage are important limitations. We propose the generation of a simulated IMU signal for pedestrians, that is obtained from a given 3D trajectory (position and attitude). The trajectory can be artificially generated or based on a real human walk pattern. This information can be used as a ground truth for the identification of systematic errors, or to obtain a statistical analysis of the effect of any noise added to the simulated signal. Any specific IMU can be simulated by adding its characteristic error pattern, and modifying them, the most influential IMU characteristics can be determined, and if possible minimized. We tested a PDR method based on an Inertial Navigation System (INS) using an Extended Kalman Filter (EKF) with a noiseless IMU signal. Since failures were detected in the stance phase, we proposed and tested some improvements. The influence of adding specific error patterns to the IMU signal were determined measuring their effect on the evolution of the standard deviation of the position error over time. The most influential source of error for an INS mechanization is the bias in the gyroscope, however the EKF-based PDR algorithm showed to diminish in a significant way many of the positioning errors. The IMU-simulation method is proposed as a way to compare several algorithms and to test new PDR improvements during algorithm design.**

***Index Terms*—Pedestrian Dead Reckoning, IMU simulation, Inertial Navigation, Extended Kalman Filter.**

I. Introduction

The latest researches in Micro Electro Mechanical (MEM) Inertial Measurement Units (IMU) has generated plenty of interest in positioning systems and in recent years there has been a lot of developments in the area of *Pedestrian Dead Reckoning* (PDR). Unlike high grade IMUs, MEM devices present an amount of bias and noise that avoids their use in pure Inertial Navigation Systems (INS). The aim of this work is to develop a method for the evaluation of the influence of each of these errors in PDR position estimations.

The development of any PDR method requires the measurement of many pedestrian trajectories, but normally there is not a ground truth to test the position errors over time. Angermann [1] proposed a IMU data set, calibrated with a video positioning system, as a reference for the error measurement and optimization of algorithms. The problem is that their displacements are limited to a given room with a finite amount of movements and a given sensor, limiting their general applicability.

978-1-4577-1804-5/11/$26.00

The error of a single trajectory is not a real measurement of the improvement of a PDR method, but just an example of a reconstruction of the position. A statistical analysis is a more complete demonstration of the capabilities of an algorithm. In [2] the variance of the position is used as a real measure of the error in the position. They only treats the effect of some accelerometer characteristics in a INS reconstruction and does not deal with the effect of the gyroscope in the positioning or the improvement of an EKF-aided mechanization. In [3] a Monte Carlo approach is proposed, based in the generation of step patterns from selections of filtered IMU measurements and from 2D visual estimation of the position of the foot, but the ground truth used is based on the INS reconstruction of the cleaned IMU signal, something that can generate some errors.

The aim of this paper is to obtain an IMU signal and its 3D position and attitude ground truth for the evaluation of any PDR method. It allows the study of the errors generated by the different characteristic error patterns of an IMU (white noise and bias in the accelerometer and gyroscope).

The paper is structured as follows. In section II we propose a simulated foot-mounted IMU signal generated from a defined basic 3D trajectory and from the fitting of a real walking pattern obtained from a motion capture system in [1]. The generated position and orientation signals are then transformed to accelerations and turn rates of the IMU. In section III an INS mechanization is tested using the generated IMU signal and the ground truth, evaluating the effect of the INS approximations and the error patterns. In section IV an INS/EKF with Zero Velocity Update (ZUPT) and Zero Angular Rate Update (ZARU) is tested (the algorithm implemented in [4]). The ground truth allowed the detection of an implementation error and two methods to correct it are proposed. After evaluating the effect of the IMU errors in the positioning, the reduction in the positioning standard deviation is shown.

II. Simulated Signals for a foot mounted IMU

The signal generation is based in the definition of a trajectory on a navigation (subindex n) frame and its transformation to the IMU body (subindex b) frame. Other external factors

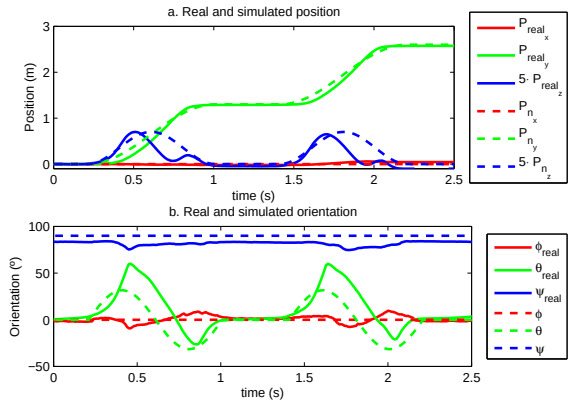

Fig. 1. Simulated two-step trajectory for a foot-mounted IMU and an equivalent trajectory obtained from a Motion Capture System in [1] (both in the navigation frame). a. Position vs. time (P_{n_z} is multiplied by 5 for an easier view) and, b. Attitude vs. time.

like magnetic fields can be modelled based on the navigation frame and then passed to the IMU body frame.

A. Basic simulated trajectory patterns in the navigation frame

To generate the reference step signal, the position $P_n = [P_{n_x}, P_{n_y}, P_{n_z}]^T$ and orientation $\Psi = [\phi, \theta, \psi]^T$ (Roll, Pitch and Yaw) of a foot mounted IMU over time are defined in a local navigation frame (North, West, Up).

Sinusoidal signals were used to generate the foot-mounted IMU trajectory during the swing phase, but any other twice-differentiable trajectory might be used. During the stance phase ($0 < t < t_0$) the position and orientation are $P_n = [0, 0, 0]^T$ and $\Psi = \Psi_0 = [\phi_0, \theta_0, \psi_0]^T$. During the swing phase ($t_0 < t < t_0 + t_u$) the basic pattern used is

$$\begin{aligned} P_{n_x} &= \tfrac{SL}{2} \cdot (1 - \cos(\tfrac{\pi \cdot (t - t_0)}{t_u})), \\ P_{n_y} &= 0, \\ P_{n_z} &= \tfrac{SH}{2} \cdot (1 - \cos(\tfrac{2\pi \cdot (t - t_0)}{t_u})), \end{aligned} \tag{1}$$

$$\begin{aligned} \phi &= \phi_0, \\ \theta &= \theta_{max} \cdot \sin(\tfrac{2\pi \cdot (t - t_0)}{t_u}) + \theta_0, \\ \psi &= \psi_o, \end{aligned} \tag{2}$$

where t_0 is the stance interval, t_u the swing interval, SL the step length, SH the step height and θ_{max} the maximal pitch.

A real trajectory obtained with a Motion Capture System ([1]) and a simulated one are observed in Fig. 1, using $t_0 = 0.4\ s$, $t_u = 0.8\ s$, $\theta_{max} = 0.55\ rad$, $SL = 1.3\ m$ and $SH = 0.14\ m$. The real trajectory was recorded moving in the Y axis, so the simulated one was rotated 90° in the Z axis

There are some differences in the swing phase between the implemented and the real signal, mainly due to the movement complexity of foot during the swing phase. In position estimation, the swing phase of an INS/EKF reconstruction is only an integrated trajectory with an error, the most critical part will be the stance phase where the step detection and filter measurements will take place.

B. Alternative Fitted Trajectory patterns in the navigation frame

For a specific simulation a more complete IMU trajectory can be implemented based on the step patterns observed with a Motion Capture System. To simplify the generation of the step patterns the position and attitude vs. time signal is treated as follows:

1) Detect the stance and swing phase to identify the steps.
2) Rotate each step pattern in the X-Y plane to align the movement in the X axis.
3) Translate each step pattern to the origin removing the initial position
4) Remove false step patterns checking his final positions and orientations.

The step patterns can be observed in the dotted lines of the Fig. 2. Due to the simplicity of the pattern we propose to fit the trajectories to a function $f(t)$ with 2 raised cosines like:

$$f(t) = A_0 \cdot (1 - \cos(2 \cdot \pi \cdot f_0 \cdot (t - t_0))) + A_1 \cdot (1 - \cos(2 \cdot \pi \cdot f_1 \cdot (t - t_1))), \tag{3}$$

for the P_{n_z}, ϕ and θ signals or with 2 half raised cosines like:

$$f(t) = A_0 \cdot (1 - \cos(\pi \cdot f_0 \cdot (t - t_0))) + A_1 \cdot (1 - \cos(\pi \cdot f_1 \cdot (t - t_1))) \tag{4}$$

for P_{n_x}.

The optimization of the values of A_0, A_1, f_0, f_1, t_0 and t_1 for each step signals $f_i(t)$ (P_{n_z}, P_{n_x}, ϕ or θ) from the step i, was achieved using the minimization of the squared error function

$$e(A_0, A_1, f_0, f_1, t_0, t_1) = \sum_i \sum_t (f_i(t) - f(t))^2 \tag{5}$$

with a Gauss-Newton and Levenberg-Mardquardt method. The generated patterns can be observed in the Fig. 2, if needed a more complete signal can be generated but for the purpose of this paper this signal and the basic trajectory defined with equations 1 and 2 are enough.

The concatenation of several straight and curved walk patterns can be used to generate a complete walking signal. To simulate a curved walk, the basic IMU trajectory during a stride is implemented using the lineal displacement P_{n_x} as an angular displacement ϑ with a constant radius r in a cylindrical reference frame $x_c = r \cdot \cos\vartheta, y_c = r \cdot \sin\vartheta$.

C. Trajectory transformation to IMU body frame measurements

The accelerations in the local navigation frame can be obtained sampling the second derivative of the position $a_n(t) = \frac{d^2 P_n(t)}{dt^2}$. The acceleration forces sensed by the IMU a_b can be obtained as a basic transformation from the accelerations in the local navigation frame a_n using the Direction Cosine matrix C_b^n. This matrix rotates a vector from the IMU body frame to the local navigation frame like $a_n = C_b^n \cdot a_b$. Adding the gravity $[0, 0, g]^T$ and solving a_b, the acceleration is

$$a_b = C_b^{nT} \cdot (a_n + [0, 0, g]^T). \tag{6}$$

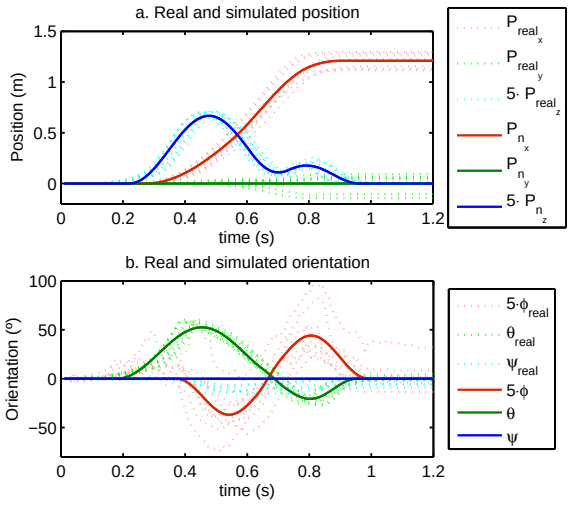

Fig. 2. Step patterns (a. Position and b. Attitude) detected with the Motion Capture System in [1] and the generated step patterns based on the minimization of the squared error.

To obtain the IMU turn rates $\omega = [\omega_x, \omega_y, \omega_z]^T$, we used the propagation of $C_b^n(t)$ expressed as

$$\frac{dC_b^n(t)}{dt} = C_b^n(t) \cdot \Omega_{nb}^b(t), \tag{7}$$

where $\Omega_{nb}^b(t)$ is

$$\Omega_{nb}^b(t) = \begin{bmatrix} 0 & -\omega_z(t) & \omega_y(t) \\ \omega_z(t) & 0 & -\omega_x(t) \\ -\omega_y(t) & \omega_x(t) & 0 \end{bmatrix}. \tag{8}$$

Assuming that the turn rates $\Omega_{nb}^b(t)$ are approximately constant in a sampling interval ΔT, then

$$C_b^n(t + \Delta T) = C_b^n(t) \cdot \exp\left(\Omega_{nb}^b(t) \cdot \Delta T\right) \tag{9}$$

and solving for the skew symmetric matrix $\Omega_{nb}^b(t)$, the values of $\omega(t)$ can be obtained from equation 8 and

$$\Omega_{nb}^b(t) = \frac{\ln(C_b^n(t)^T \cdot C_b^n(t + \Delta T))}{\Delta T}. \tag{10}$$

The real IMU signal from [1] can be seen in Fig. 3, rotated to have the gravity during the stance in the Z axis and move in the X axis. The obtained noise-free accelerometer and gyroscope signals in the body frame from the basic trajectory can be observed in Fig. 4, it was generated for a straight walk with $SL = 1.3\ m$, $SH = 0.14\ m$, $\theta_{max} = 0.55\ rad$, $t_0 = 0.4\ s$, $t_u = 0.8\ s$ and $\Psi_0 = [0, 0, 0]^T$. The IMU signals generated from the fitted trajectory patterns are shown in Fig. 5.

As it can be seen the signal generated from the fitted trajectory is closer to the real accelerations and turn rates. Although a more realistic signal can be implemented, for the purpose of this work the basic and the position based signals are enough.

Other authors propose a separated position estimation and IMU measurements, but errors in the synchronization of the

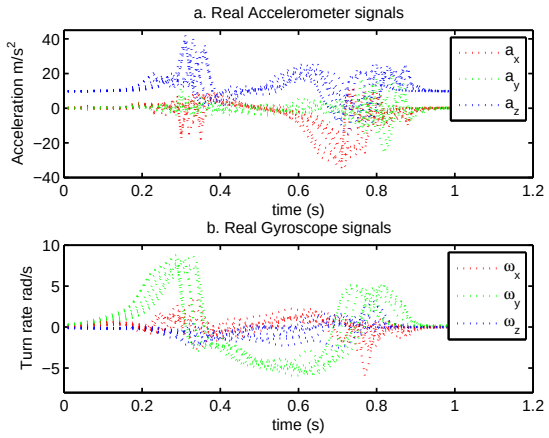

Fig. 3. Real accelerometer (a) and gyroscope (b) signals (in the body frame) of recorded steps from [1] rotated to have the gravity in the Z axis during the stance and move in the X axis.

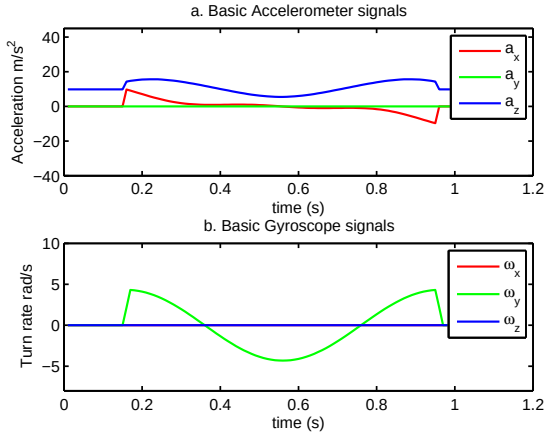

Fig. 4. Simulated accelerometer (a) and gyroscope (b) signal (in the body frame), using the basic trajectory for a foot-mounted IMU along a straight line walk, equations 1 and 2.

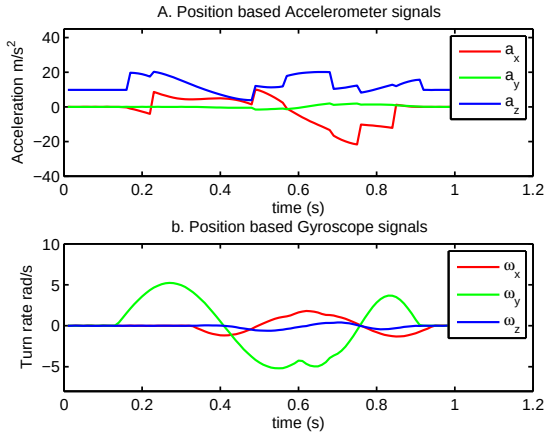

Fig. 5. Simulated accelerometer (a) and gyroscope (b) signal (in the body frame), using the fitted trajectory patterns for a foot-mounted IMU along a straight line walk, equations 3 and 4

devices and the added noise of each measurement limits the error detection of the signal. The IMU signal with its ground truth presented in this works allows statistical analysis of the evolution of the error over time, allowing a better understanding of the influence of each error source.

Several generated IMU signal and their ground truth trajectories, including straight, circular and mixed walks, will be available in our webpage for other PDR developers to evaluate their algorithms.

III. Evaluation of an INS Mechanization

The INS mechanization is the simplest position reconstruction algorithm based on the signals of an IMU. As it is known it has the following steps:

1) Propagate the attitude from the gyroscope signal, using equation 9.
2) Obtain the acceleration in the local navigation frame, solving from equation 6.
3) Integrate the acceleration twice to obtain the velocity and position of the system.

Using the data generated in section II as a ground truth, different attitude propagations methods are evaluated. The effects of the IMU errors are tested and compared with [2].

A. Testing different INS attitude propagations methods

The effect of the approximations of the exponential (equation 9) was evaluated using a noiseless simulated signal, generated at several sampling frequencies. Some INS implementations use a [1,1] Padé approximant like

$$\text{Padé}[1,1]\{\exp(\Omega_{nb}^b \cdot \Delta T)\} = \frac{2 \cdot I + \Omega_{nb}^b \cdot \Delta T}{2 \cdot I - \Omega_{nb}^b \cdot \Delta T}, \tag{11}$$

other implementations, such as [5], uses the fact that Ω_{nb}^b is skew symmetrical and simplifies the equation to a sinusoidal representation of the form:

$$\exp(\Omega_{nb}^b \Delta T) = I + \frac{\sin(\|\omega \Delta T\|)}{\|\omega\|}\Omega_{nb}^b + \frac{(1-\cos(\|\omega \Delta T\|))}{\|\omega\|^2}{\Omega_{nb}^b}^2. \tag{12}$$

The error in the final position of a straight walk was used to evaluate the different approximations to the attitude determination of the INS mechanization. In this test several Padé approximants ([1,0], [1,1], [2,1], [2,2] and [3,3]), the sinusoidal representation and the function expm of MATLAB (a [6,6] Padé approximant with scaling and squaring) were proposed for the computation of equation 9. This approximations were evaluated at some common sampling frequencies: 10, 20, 40, 100, 200, 400 and 1000 Hz.

Results are shown in Fig. 6, for a 10 step (13 m) straight walk simulation with the characteristics of the ones used in Fig. 4. The best solutions are obtained with Padé [2,2], [3,3], the sinusoidal representation and expm(), being Padé [2,2] and the sinusoidal representation the less computationally expensive.

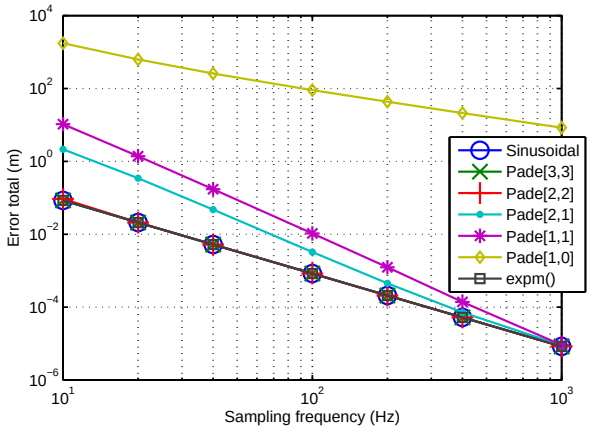

Fig. 6. Position error of an INS mechanization for different approximations for the attitude propagation. Study performed over a 10 step (13 m) straight walk with a basic pattern

B. Influence of the IMU noise in the INS mechanization

Several errors were added to the simulated signal to evaluate their influence on the INS mechanization. We included white noise (random walk) and a random constant (bias). Other more complex models such as flicker noise (normally associated with the bias instability) or even Gauss-Markov or Periodic random processes ([6]) will be studied in the future. In a human walk pattern the characteristics of the steps change between each other, they can be simulated generating those parameters randomly, but for the purpose of this study we are only evaluating the effects of the IMU errors.

One thousand simulations were made with several noise levels, changing the standard deviation, σ, of the random variable in the Accelerometer noise, Accelerometer bias, Gyroscope noise and Gyroscope bias. The effect of each noise was associated with the measured root mean squared error over time of the position (σ_p),

$$\sigma_p(t) = \sqrt{\frac{1}{N} \cdot \sum_{i=1}^{N} (P_{n,i}(t) - P_n(t))^2} \tag{13}$$

and the yaw (σ_y)

$$\sigma_y(t) = \sqrt{\frac{1}{N} \cdot \sum_{i=1}^{N} (\psi_i(t) - \psi(t))^2}, \tag{14}$$

where $P_{n,i}(t)$ and $\psi_i(t)$ are the obtained position and attitude from the simulation i of N, and $P_n(t)$ and $\psi(t)$ are the ground truth. Using a logarithmic scale and approximating to a line, the models of the Standard Deviations increment with time were obtained (Table I).

It is shown that the most influential source of error in an INS mechanization is the gyroscope. This is due to the fact that they generate an attitude error and therefore a wrong estimation of the gravity orientation, a double integrated source of error.

IMU Error introduced	σ_p	σ_y
Accelerometer noise	$0.1 \cdot \sigma \cdot t^{1.5}$	0
Gyroscope noise	$0.3169 \cdot \sigma \cdot t^{2.5}$	$0.1 \cdot \sigma \cdot t^{0.5}$
Accelerometer bias	$\sigma \cdot t^2$	0
Gyroscope bias	$2 \cdot \sigma \cdot t^3$	$\sigma \cdot t$

TABLE I
SIMULATED POSITION'S AND YAW'S ROOT MEAN SQUARED ERROR INCREMENT OVER TIME AS A FUNCTION OF THE KIND AND LEVEL OF NOISE INTRODUCED TO THE IMU, σ, IN A INS MECHANIZATION

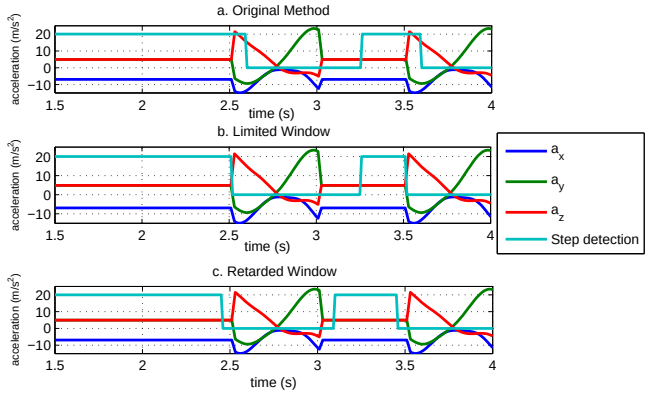

Fig. 7. Comparison of different stance detection methods for PDR INS/EKF mechanization: a. Original Method. b. Limited Window. c. Retarded Window

IV. EVALUATION OF A INS/EKF PDR ALGORITHM

An IMU signal was introduced to the PDR method proposed in [4] with ZUPT and ZARU corrections but without the magnetometers measurements. The method was verified with the basic noiseless signal and the influence of the IMU errors was tested by simulating several noise conditions.

A. Noiseless IMU signal evaluation/ Stance detection improvement

After evaluating the position estimates with the basic noiseless simulated IMU signal, the EKF showed an increasing error in the direction of the movement. The test showed that it was generating a false stance detection during the initial samples of the swing phase as shown in Fig. 7.a. The original Stance detection algorithm is implemented as:

$$C_1(k)=th_{a_{low}}<\|a(k)\|<th_{a_{high}}, \quad (15)$$

$$C_2(k)=\|\omega(k)\|<th_{\omega}, \quad (16)$$

$$C_3(k)=\sigma(a(k-W1{:}k))<th_{\sigma}, \quad (17)$$

$$Conditions(k)=C_1 \cdot C_2 \cdot C_3, \quad (18)$$

$$Stance(k)=median(Conditions(k-W2{:}k)), \quad (19)$$

where $\sigma(a(k-W1 : k))$ is the standard deviation of the acceleration magnitude over the last W1+1 samples and $median(Conditions(k-W2:k))$ is the median filter of the conditions over the last W2+1 samples.

The problem presented is due to the median filter used to detect the stance and still phases. When the foot start moving, the median filter keep the stance phase until more than half the "not stance" conditions are in the evaluation window, prolonging the stance phase.

Two solutions are proposed to compensate the problem:

1) The limited window step detection (Fig. 7.b) add an additional $Conditions(k)$ check at any point believed to be a Stance (multiplying by $Conditions(k)$ in the equation 19).
2) The retarded window solution (Fig. 7.c) use W1=W2=W and delay the measurements W/2 samples. This way the median filter of equation 19 has a window of W+1 samples centered at the time of the measures of the EKF, avoiding a delay in the detection of the stance with respect to the provided signal but adding a delayed and more complex algorithm.

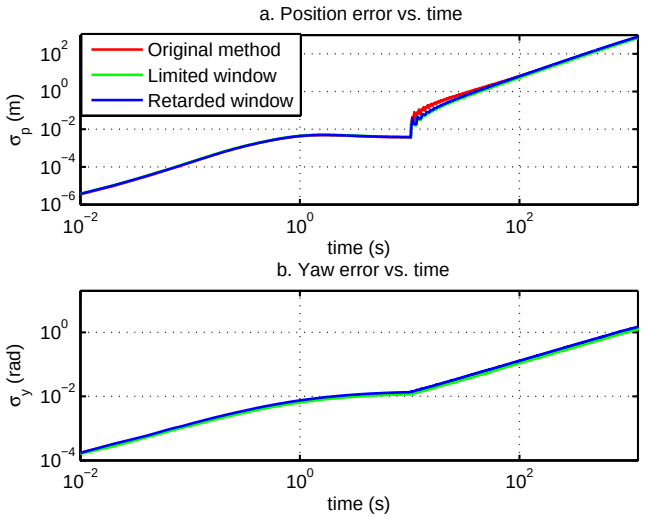

Fig. 8. Evolution of the root mean squared error over time (a. Position, b. Yaw) for the different step detection methods for an IMU signal with all the errors included

B. IMU Noise influence in the PDR INS/EKF method

To evaluate the EKF algorithm it was provided an IMU signal that during the first 10 seconds was motionless, and after that performs a 1000 step straight walk, with the same pattern used for Fig. 5 and the characteristic noise of a XSense MTi ($3\ ^\circ/\sqrt{hr}$ angular random walk and $122\ \mu g/\sqrt{Hz}$ velocity random walk), the constant bias components were generated using 3 random values (one for each axis) with a Gaussian distribution for the accelerometer (standard deviation of 1.23 mg) and the gyroscope (standard deviation of 0.5 °/seg).

The root mean squared error over time of the position σ_p and the yaw σ_y were used to measure the evolution of the error for each step detection method. In Fig. 8 the errors are observed after 100 simulation with all the error patterns.

The algorithm make ZUPT and ZARU corrections at the initial phase of the trajectory (as it can be seen the error stabilize around 10^{-2} m and 10^{-2} rad during the first 10 seconds) and then ZUPT corrections during the stance phases

IMU Error introduced	Original Method	Limited Window	Retarded Window
Accelerometer noise	$2 \cdot 10^{-2} \cdot t^{1.11}$	$6 \cdot 10^{-4} \cdot t$	$3 \cdot 10^{-4} \cdot t$
Gyroscope noise	$3 \cdot 10^{-2} \cdot t + 1.5 \cdot 10^{-4} \cdot t^2$	$2 \cdot 10^{-3} \cdot t + 1.5 \cdot 10^{-4} \cdot t^2$	$2 \cdot 10^{-3} \cdot t + 1.5 \cdot 10^{-4} \cdot t^2$
Accelerometer bias	$3 \cdot 10^{-1} \cdot t + 10^{-4} \cdot t^2$	$10^{-3} \cdot t + 3 \cdot 10^{-6} \cdot t^2$	$10^{-3} \cdot t + 2 \cdot 10^{-6} \cdot t^2$
Gyroscope bias	$3 \cdot 10^{-2} \cdot t + 6 \cdot 10^{-4} \cdot t^2$	$1.3 \cdot 10^{-2} \cdot t + 6 \cdot 10^{-4} \cdot t^2$	$1.3 \cdot 10^{-2} \cdot t + 6 \cdot 10^{-4} \cdot t^2$

TABLE II
SIMULATED POSITION'S ROOT MEAN SQUARED ERROR INCREMENT OVER TIME AS A FUNCTION OF THE KIND OF NOISE INTRODUCED TO THE IMU AND THE STEP DETECTION METHOD IN A INS/EKF PDR MECHANIZATION

IMU Error introduced	Original Method	Limited Window	Retarded Window
Accelerometer noise	$2 \cdot 10^{-4} \cdot t$	$5 \cdot 10^{-6} \cdot t$	$7 \cdot 10^{-7} \cdot t + 6 \cdot 10^{-9} \cdot t^2$
Gyroscope noise	$2.7 \cdot 10^{-4} \cdot t$	$2.3 \cdot 10^{-4} \cdot t$	$2.3 \cdot 10^{-4} \cdot t$
Accelerometer bias	$2 \cdot 10^{-4} \cdot t$	$6 \cdot 10^{-6} \cdot t$	$1.3 \cdot 10^{-7} \cdot t$
Gyroscope bias	$1.25 \cdot 10^{-3} \cdot t + 10^{-2}$	$1.25 \cdot 10^{-3} \cdot t + 10^{-2}$	$1.25 \cdot 10^{-3} \cdot t + 10^{-2}$

TABLE III
SIMULATED YAW'S ROOT MEAN SQUARED ERROR INCREMENT OVER TIME AS A FUNCTION OF THE KIND OF NOISE INTRODUCED TO THE IMU AND THE STEP DETECTION METHOD IN A INS/EKF PDR MECHANIZATION

of each step. It is seen that the new step detection methods have a minor improvement over the original method in the first seconds of the walking time, but after some time all the methods converge to the same tendency.

To observe the effect of each noise source on the position and orientation error the simulations were repeated adding only one source at a time. The main tendencies for the errors are shown in table II (σ_p) and table III (σ_y), using the values of the error during the stance phase.

There are two noise sources of particular interest, the accelerometer noise (Fig. 9) and the gyroscope bias (Fig. 10, in both figures the initial 10 seconds motionless phase were removed to observe only the walking phase). In the first the proposed step detection methods generates errors significantly lower than the original method. In the last, generates similar error patterns for all the methods due to the quick lost of the heading observed and reveals the need of yaw information.

The Kalman filter shows a diminishing of the order of the error generated in a pure INS system, but generates the lost of the heading even without any noise in the gyroscope. With the use of heading information like a Magnetometer this limitation can be eliminated.

V. CONCLUSIONS

We have presented a method to obtain a simulated IMU signal from a trajectory in a local navigation frame. Using a basic pattern or approximating to an observed one, IMU signals are obtained to evaluate different Dead Reckoning algorithms. The basic signals can be contaminated with a

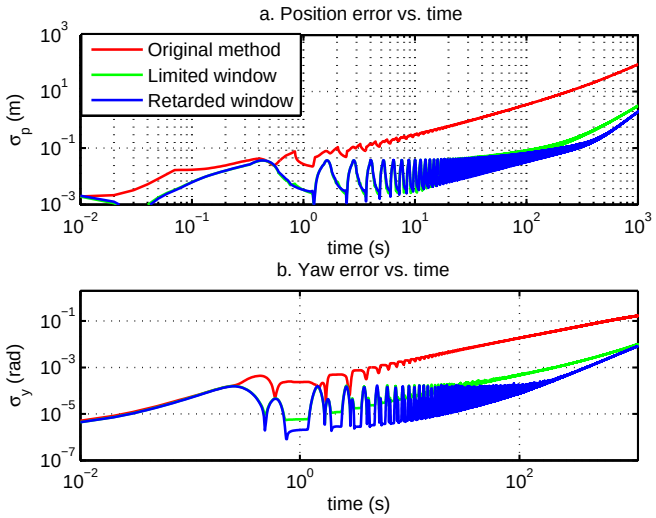

Fig. 9. Evolution of the root mean squared error over time (a. Position, b. Yaw) for the different step detection methods for an IMU signal with added accelerometer noise.

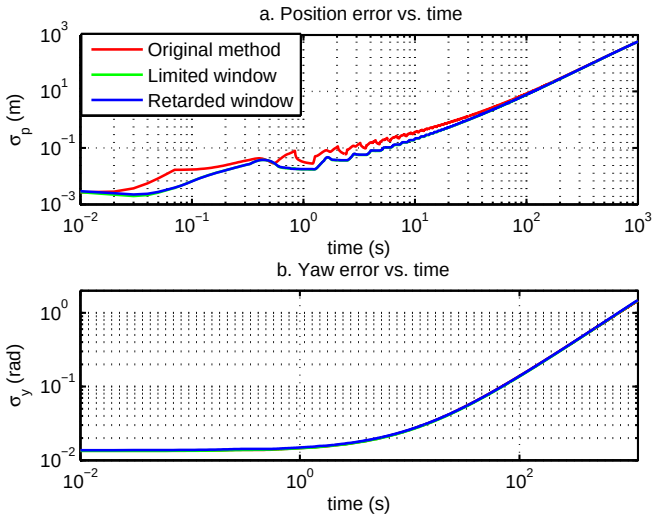

Fig. 10. Evolution of the root mean squared error over time (a. Position, b. Yaw) for the different step detection methods for an IMU signal with added gyroscope bias.

given noise or error to evaluate his influence in the INS mechanization or PDR INS/EKF

The simulated signal was used to evaluate an INS position estimation and the different effects of the INS approximations and the sensor's sampling frequency. It can be observed that the main source of error in a INS mechanization is the bias of the gyroscope.

In the PDR INS/EKF algorithm, the simulated IMU signal allowed us to observe a false step detection problem and to correct it proposing two different strategies (limited window and retarded window). The algorithm was tested with different error patterns and it is shown that the proposed methods minimize the errors in some conditions, but the lost of

the heading (an unobservable state with the measures) still generates a second order error that needs to be corrected.

ACKNOWLEDGMENT

The authors thanks the financial support received from projects: LEMUR (TIN2009-14114-C04-03) and LAZARO (CSIC-PIE Ref.201150E039).

REFERENCES

[1] M. Angermann, P. Robertson, T. Kemptner, and M. Khider, "A High Precision Reference Data Set for Pedestrian Navigation using Foot-Mounted Inertial Sensors," in *2010 International Conference on Indoor Positioning and Indoor Navigation (IPIN), 15-17 September 2010, Zürich, Switzerland*, no. September, p. 6, 2010.

[2] J. H. Wall and D. M. Bevly, "Characterization of Inertial Sensor Measurements for Navigation Performance Analysis," *Proceedings of ION GNSS*, pp. 1–8, 2007.

[3] C. Ascher, C. Kessler, A. Maier, P. Crocoll, and G. Trommer, "New pedestrian trajectory simulator to study innovative yaw angle constraints," in *Proceedings of the 23rd International Technical Meeting of The Satellite Division of the Institute of Navigation (ION GNSS 2010)*, pp. 504–510, September 2010.

[4] A. Jimenez, F. Seco, J. Prieto, and J. Guevara, "Indoor Pedestrian Navigation using an INS/EKF framework for Yaw Drift Reduction and a Foot-mounted IMU," in *WPNC 2010: 7th Workshop on Positioning, Navigation and Communication*, vol. 10, 2010.

[5] D. Titterton and J. Weston, *Strapdown Inertial Navigation Technology*. 2004.

[6] S. Nassar, *Improving the Inertial Navigation System (INS) Error Model for INS and INS / DGPS Applications*. PhD thesis, 2003.